ELSEVIER

Nuclear Instruments and Methods in Physics Research B 133 (1997) 15–23

NIM B
Beam Interactions with Materials & Atoms

The "invisible" metal particles in catalysis

Sofía Díaz-Moreno [a], D.C. Koningsberger [b], Adela Muñoz-Páez [a,*]

[a] *Departamento de Química Inorgánica, Instituto de Ciencias de Materiales, Centro mixto CSIC-Universidad de Sevilla, ClAmerico Vespuccio s/n, Isla de la Cartuja, 41092-Sevilla, Spain*

[b] *Laboratory of Inorganic Chemistry and Catalysis, Debye Institute, University of Utrecht, P.O. Box 3508, TB Utrecht, The Netherlands*

Abstract

An easy, reliable and straightforward method to determine the sizes of small metal particles in supported metal catalyst which are invisible for most techniques (chemisorption, XRD, HRTEM) is presented. The technique we consider more appropriate is EXAFS, because it detects metal–metal bonds even before metal atoms are forming particles. Due to this capability it has become a routine technique in catalysis, although it requires an elaborate data analysis procedure. In the particular case of supported metal catalyst, this procedure can be simplified because nearly everything is known about the investigated structure, the metal particles. With the appropriate fitting strategies, the main contribution to the EXAFS spectrum, the metal–metal bonds, can be emphasized, and within it, most part of the fit parameters are known. The only unknown parameter is the coordination number for each metal shell. Once this value is obtained, the number of metal atoms per particle can be calculated and from that, metal particle diameter can be deduced. An example of this procedure for a Pt/Al_2O_3 catalyst is shown. © 1997 Elsevier Science B.V.

Keywords: Metal catalyst; EXAFS; Dispersion; Pt/Al_2O_3

1. Introduction

During the last decade there has been an exponential growth of the use of EXAFS in catalysis [1], that can be clearly appreciated, for instance, by reviewing the general indices of the Journal of Catalysis during this period. Within this field, one of the most widespread applications of EXAFS has been the determination of metal dispersions in supported catalysts. Nearly everybody working in heterogeneous catalysis has met some articles where metal particle sizes are determined using EXAFS.

The first systematic approach to this type of studies was carried out by Lytle and Greegor [2] and published in 1980. In this study they relate the EXAFS parameters obtained for several systems with the values deduced for discs, cubes and sphere-shaped metal particles. Since then, many additional contributions have appeared, data analysis have been refined, data quality has improved and EXAFS has become a widespread method for determining particle diameter in highly dis-

*Corresponding author. Tel.: +34 5 4557164; fax: +34 5 4557134; e-mail: adela@cica.es.

PII S0168-583X(97)00461-8

persed metals. Although a high number of papers include particle diameters determined from EXAFS, it is not a "standard" method, and the results obtained with it can be contradictory. We believe the reason is the complexity of data analysis, as compared to other structural techniques, and the existence of some conflicting points.

Herein we will illustrate how the information about the structure of very small metal particles can be obtained in a straightforward way using a technique that yields unique information. We will use some of our results to show how data analysis can be simplified for this special type of systems, the supported metals, because metal atoms have a strong tendency to bind following always the same pattern, that of the stable crystalline phase. Thus, coordination distances, may, without certain limits, i.e. a few hundredths of an angström, be anticipated.

Prior to this, we will refer briefly to the reasons that render metal dispersion determination so important in heterogeneous catalysis. We will mention as well the relation between coordination number for metal–metal bonds and metal particle sizes, according to the different models.

We will finish by summarizing the conflicting points in the application of EXAFS to metal particle size determination and the way of overcoming them.

2. Heterogeneous catalyst and metal dispersion determination: XRD, TEM and chemisorption methods

Heterogeneous catalysts are generally formed by an active phase, usually a noble metal, dispersed over a supporting oxide of high specific area (>100 m^2/g) [3]. The unique entities active in the heterogeneous catalytic processes are the metal atoms from the surfaces, edges or corners. Since the active phase is very expensive, one of the main goals of catalyst preparation is achieving the highest ratio surface metal atoms to total metal atoms [4]:

$$N_{\text{surface atoms}}/N_{\text{total atoms}} = D \qquad (1)$$

This ratio, D, is known as metal dispersion. To obtain the highest metal dispersion very small metal particles are required, with a diameter on the order of or smaller than 50 Å. To succeed in preparing a good heterogeneous catalyst, a quick and reliable method for determining metal dispersions is needed. Moreover, knowing D, the rate of a catalytic reaction per exposed surface metal atom, the turnover number, TON, can be obtained. This parameter allows the quantitative comparison of catalytic activities.

A standard method for obtaining structural information, X-ray diffraction, is appropriate but has some limitations. First of all, it requires the arrangement of atoms in the small particles in an ordered way to yield coherent diffraction peaks. Secondly, the decrease of particle sizes produces a widening in the diffraction peaks that, according to the Scherrer equation [5], scales as

$$b = k\lambda/(d \cos \theta), \qquad (2)$$

where b is the line width in degrees, θ the diffracting angle, d the mean diameter of the diffracting particle, λ the X-ray wavelength, and k is a constant with a value of ca 57. Thus for $\lambda = 1.5$ Å and metal particles of 30 Å diameter on average, the width of the main diffraction peak is around 3°, too high for quantitative determinations.

Due to these limitations, chemisorption methods have been used to determine metal dispersions [6]. In this method, it is assumed that a given gas, typically H_2 or CO, is irreversible and selectively adsorbed onto the metal surface atoms with a given stoichiometry. Determining the number of gas moles adsorbed by a known amount of catalyst, the metal dispersion is calculated. Complex phenomena, such as the so-called "strong metal-support interaction" [7] that causes a drastic decrease in the chemisorption capacity of the supported metals, or the "spillover" [8] of the adsorbed gas to the support surface, can make unreliable the values of metal dispersion D obtained with this method. Moreover, the maximum dispersion, 1, is reached for particle sizes of around 10 Å. Below this size, chemisorption cannot discriminate between different particle sizes.

With conventional transmission electron microscopy metal particles 15–20 Å in diameter can be detected and size distribution can be obtained because, in contrast with other techniques, TEM does not provide average values, but independent

information about each particle. With HRTEM, particles as small as 8 Å can be detected [9]. As in XRD, metal atoms have to be arranged in an ordered way, and electron micrographs have to be recorded under vacuum, while EXAFS can be recorded "in situ" and at reaction conditions. Moreover, while recording TEM micrographs, the very small metal particles can be damaged with the beam. And again, the low limit for metal particle detection is too high to study the metallic phase of highly dispersed catalysts.

How the metal particles below 10–15 Å in diameter, "INVISIBLE" for most techniques can be detected and their sizes determined?

3. Average coordination number for small metal particles

For these very small metal particles the coordinatively unsaturated (cus) atoms from edges, corners and surfaces represent a nonnegligible fraction, and consequently, their average coordination numbers are smaller than in bulk metals. The accurate determination of these coordination numbers is the key for knowing their sizes.

What are bulk values of coordination numbers and how do they change in small metal particles?

Most catalytically active metals have close packed structures, either cubic (face centered cubic, fcc) or hexagonal close packed (hcp) [10]. Coordination numbers for bulk atoms showing fcc structures are 12, 6, 24, 12 for the first, second, third and fourth coordination shells, respectively. These numbers, on average, remain constant in medium and large metal particles. But for the small ones, the number of cus atoms is significant, and thus the average coordination number for the first and higher shells decreases.

The variation of these coordination numbers is directly related to the size and shape of metal particles, as shown in the Fig. 1, where average coordination number for the first shell has been plotted against the number of metal shells in the particle, for spheres, cuboctahedra and icosahedra. The curves have been calculated with the expression proposed by Benfield [11]. Metal particles are usually assumed to have spherical shapes, although a more accurate approximation is considering them as cuboctahedra. As can be seen in the plot, there are no big differences for small metal particles, but for medium and large particles, coordination number for spheres are always higher. For these sizes the spherical shape becomes rather inaccurate. Other authors have proposed similar expressions correlating metal particle diameter and number of atoms [2,12–14].

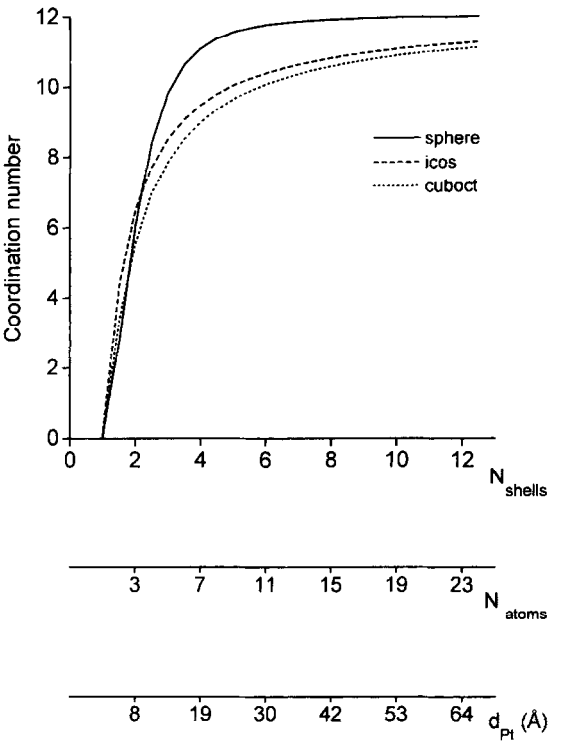

Fig. 1. Variation of first shell coordination number in spheres, cuboctahedron and icosahedron versus number of metal shells, number of metal atoms per particle, and versus diameter of platinum particles in angströms.

Similarly, the variation of coordination number for higher shells can be calculated. In the same way, there is a direct relationship between the number of metal atoms and particle diameter. Thus, if a given technique is able to detect metal–metal bonds from the moment they are formed, light will be shed on the invisible metal particles: This is exactly what EXAFS does.

Here we will show an example of particle size determination from EXAFS spectra, indicating

some strategies to simplify the analysis. Afterwards the conflicting points in the application of EXAFS to these systems will be discussed.

4. Metal particle sizes in Pt/Al_2O_3 catalysts

As a practical example we will show how metal particle sizes were determined in a catalyst prepared by incipient wetness of an alumina support with an aqueous solution of the Pt^{2+} complex $[Pt(NH_3)_4](OH)_2$ [15]. Once deposited, the complex was either directly reduced at 350°C (sample R350) or dried under He at 120°C and then reduced at increasing temperatures, being the higher 350°C (sample DECH350), or calcined in the air at 350°C and then reduced at 350°C (sample OR350) as shown in Fig. 2. The prereduction treatments had drastic effects on metal particle size.

Standard procedures were used to generate the EXAFS spectrum from the experimental absorption spectrum. Normalization was done by dividing by the height of the absorption edge and the background was subtracted using cubic spline routines. The errors in the structural parameters were calculated from the covariance matrix taking into account the statistical noise of the EXAFS data and the correlations between the different coordination parameters. The values of the goodness of fit (ϵ_ν^2) were calculated as outlined in the Reports of Standard and Criteria in XAFS Spectroscopy. Reference phase shift and backscattering amplitude functions for Pt–O, Pt–N and Pt–Pt absorber–backscatter pairs were determined from the EXAFS spectra of $Na_2[Pt(OH)_6]$, $Pt(NH_3)_4(OH)_2$ and Pt foil, respectively. Further details and additional references can be found in Ref. [15].

The plots included in Fig. 3(a) show the EXAFS spectra of the $[Pt(NH_3)_4](OH)_2/Al_2O_3$ sample

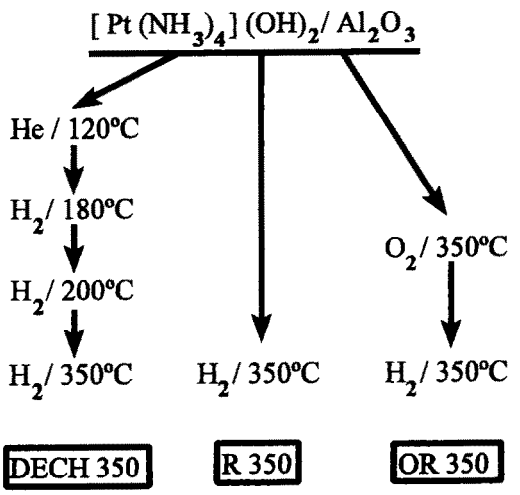

Fig. 2. Treatments given to samples DECH350, R350 and OR350 obtained from the decomposition of a $[Pt(NH_3)_4](OH)_2/Al_2O_3$ precursor.

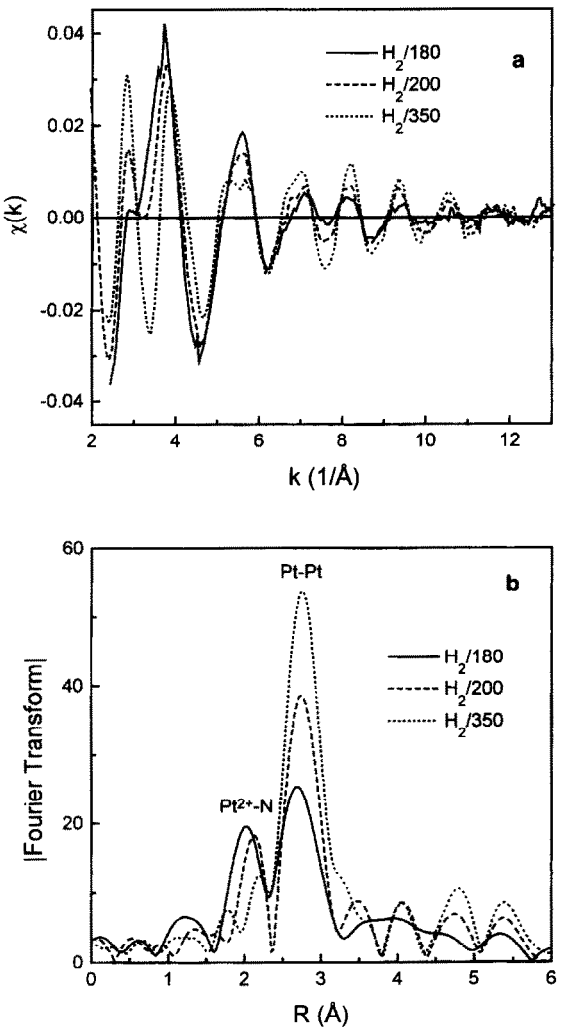

Fig. 3. (a) EXAFS spectra of samples DECH180, DECH200 and DECH350. (b) Magnitude of the phase and amplitude corrected Fourier transform of the EXAFS spectra of part (a).

recorded after the in situ treatment under hydrogen at increasing temperatures. The magnitude of the corresponding Fourier transforms appears in Fig. 3(b). For the freshly prepared catalyst, the main contribution to the EXAFS signal is that due to species $[Pt(NH_3)_4]^{2+}$ with four Pt^{2+}–N bonds. The amplitude of Pt–Pt contribution increases with reduction temperature, while that of Pt^{2+}–N decreases. At the same time, higher Pt–Pt shells appear. For all samples the full reduction of Pt is only achieved after treatments under hydrogen at 350°C. After reduction at lower temperatures platinum metal is not fully reduced, and thus the obtained coordination numbers have to be corrected taking into account the fraction of oxidized platinum. We will not consider these systems.

The fitting parameters obtained for the spectra of the fully reduced samples appear in Table 1. The directly reduced sample (R350) shows the highest Pt–Pt coordination numbers, indicating it has the largest metal particles, while the calcined one (OR350) shows the smallest.

Reaching this point, to simplify the fitting procedure and since the contribution to the EXAFS spectrum of the first metal–metal shell is the most intense, many authors isolate it, and fit the Fourier filtered data. In this way, they neglect useful information from higher Pt–Pt coordination shells that complement and confirm that obtained from the first shell.

We propose an alternative way of simplifying the data analysis. First, it has to be taken into account that the final structure is well known, bulk fcc metal, which renders the analysis straightforward if the appropriate information is used. This is the case of samples DECH350 and R350, where only Pt–Pt_n ($n = 1$–4) contributions have been considered. For them, coordination distances are known, the Debye–Waller factors for metal samples measured at liquid nitrogen temperature range between 0.002 and 0.006 Å^2, and they should decrease with the increase of metal particle size (that is N); they should be minimum in the largest metal particles, where metal atoms are better ordered than in the smaller ones.

In the calcined sample, OR350, data analysis is more delicate because it includes Pt–O contributions from the interface. For small metal particles, around 10 Å in diameter, these contributions cannot be neglected, because it would lead to wrong N and $\Delta\sigma^2$ values for Pt–Pt contributions. Fig. 4 includes the Fourier filtered experimental spectrum and the best fit obtained discarding these contributions. Since the contributions of the metal-support were being investigated in this system, this fit was carried out with k^1 weighting, to emphasize Pt–O contributions. On the contrary, if we want to emphasize metal–metal contributions, we should use a higher weight. Additional differences between low-Z scatterer and high-Z scatterer is the

Table 1
EXAFS coordination parameters for Pt–Pt_n ($n = 1$–3) for fully reduced samples [a]

Parameters	N	$\Delta\sigma^2$ (Å)$^2 \times 10$	R (Å)	ΔE_0 (eV)
Coordination Pt–Pt_1				
DECH350	7.2 (0.3)	3.0 (0.5)	2.770 (0.004)	3.3 (0.4)
R350	10.1 (0.2)	2.0 (0.1)	2.771 (0.001)	3.8 (0.2)
OR350	5.5 (0.3)	3.0 (0.3)	2.775 (0.003)	2.5 (0.5)
Coordination Pt–Pt_2				
DECH350	2.8 (1.5)	5.7 (6.7)	3.90 (0.04)	−4.3 (3.1)
R350	4.4 (0.5)	2.4 (1.1)	3.93 (0.01)	−5.0 (1.0)
OR350	2.0 (0.3)	3.0 (1.3)	3.96 (0.01)	−8.5 (0.7)
Coordination Pt–Pt_3				
DECH350	8.8 (3.6)	8.2 (6.5)	4.79 (0.04)	1.0 (2.4)
R350	17.5 (1.1)	2.8 (0.6)	4.78 (0.01)	3.3 (0.6)

[a] Taken from Ref. [15].

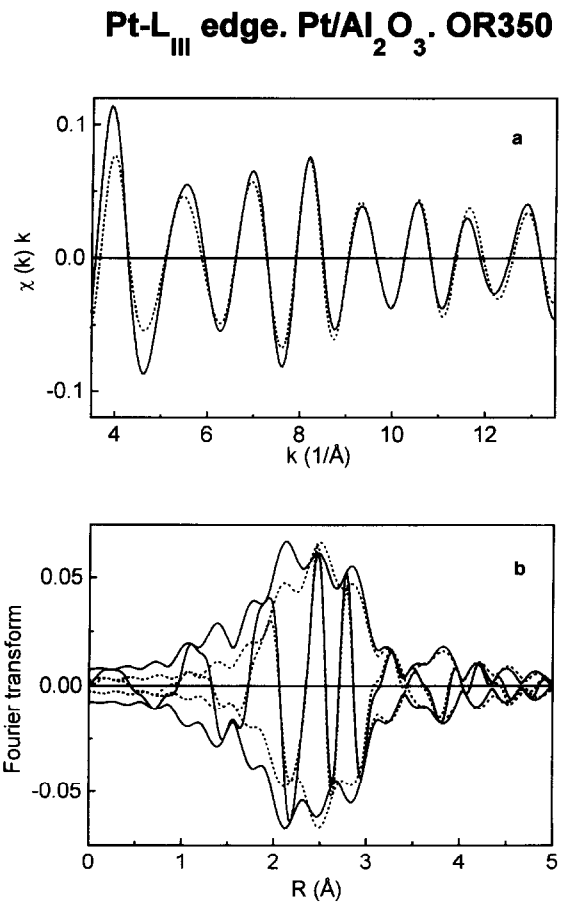

Fig. 4. EXAFS spectrum and best fit of sample OR350 including only Pt–Pt$_n$ ($n=1$, 2) contributions. k^1 fit, $\Delta k = 3.5$–13.5 Å^{-1}, $\epsilon_v^2 = 9.2$

dependence of the backscattering amplitude, $F(k)$, with the wave vector, k. In Fig. 5, backscattering amplitude functions for Pt–Pt and Pt–O contributions calculated with the parameters of Table 2 have been plotted. At high k, $F(k)$ for Pt–O is negligible, while Pt–Pt backscattering amplitude is

Table 2
Parameters used for calculating Pt–Pt and O–O backscattering amplitude functions

	R (Å)	σ	λ	S_0^2
Pt–Pt	2.774	0.000	6.00	1.00
O–O	2.050	0.000	10.00	1.00

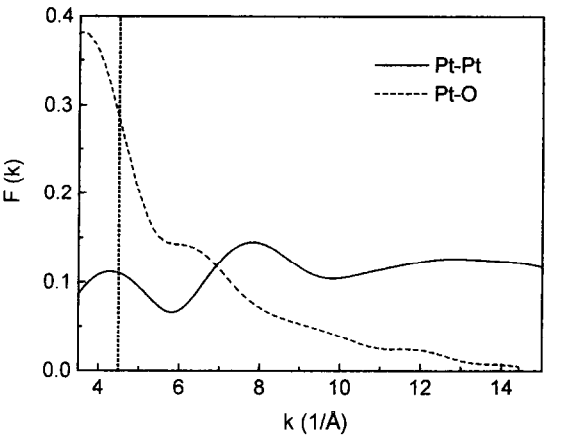

Fig. 5. Backscattering amplitude function for Pt–Pt and Pt–O contributions.

dominant. Thus Pt–Pt contributions can be emphasized shifting the k range of the fit to high k values. The effect of increasing k weight to k^2, and shifting fit range to $\Delta k = 4.5$–13.5 Å^{-1} in sample OR350 appear in Fig. 6. The fit has improved considerably although Pt–O contributions from the interface have been discarded. All the other fit parameters have been kept identical.

With this strategy and using as input values for $\Delta\sigma^2$, R and ΔE_0 those of the corresponding metal foil measured at the same temperature, one can obtain an approximate value of coordination numbers of the first and higher shells very easily. In some systems, multiple scattering phenomena often compromise the reliability of the information extracted from higher coordination shells. We have discussed extensively this issue in other type of systems elsewhere [16,17]. For platinum particles MS contributions are relevant in the fourth coordination shell, where Pt atoms are aligned with those from the second shell. Because of this, we are not including this shell here.

The number of metal atoms in the particle can be calculated independently from the values of the coordination number of each metal shell. The agreement between the obtained values can inform about the consistency of the method. Additionally, it informs about metal particle shape. For instance, the lack of the second coordination shell while the third is present, indicates that metal

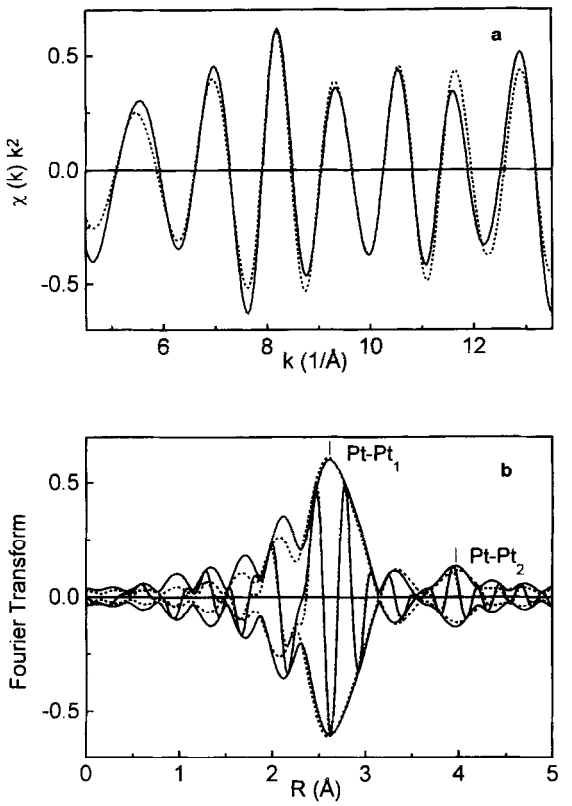

Fig. 6. EXAFS spectrum and best fit of sample OR350 including only Pt–Pt$_n$ ($n=1$, 2) contributions. k^2 fit, Δk = 4.5–13.5 Å^{-1}, $\epsilon_v^2 = 2.6$

particles are raft-like [18]. The values obtained for the fully reduced samples from the three first coordination shells have been included in Table 3. For sample DECH350 and OR350 similar values of metal particle diameter are obtained from the three shells, indicating a very consistent fit.

Additional examples where metal particle sizes are deduced from EXAFS coordination numbers can be found in Refs. [15,19–21].

5. Conflicting points

There is a series of limitations of the technique that have to be taken into account when using it. Some of them are inherent to the technique, some others are related with the investigated system. They can be summarized as follows.

1. The technique provides average values.
2. Several factors affect the EXAFS function amplitude:
   - Amplitude reduction factor, S_0^2 [22].
   - The Debye–Waller factor.
   - Coordination number.

For supported metals

1. The anharmonic contribution to the pair distribution function is not negligible [12,23].
2. For very small metal particles there seems to be a bond length contraction [24].
3. For partially oxidized metals a correction factor has to be used to obtain real coordination numbers [25].

In relation with the first point, nothing can be done because it is characteristic of the technique providing average radial information. As a consequence particle size distributions cannot be obtained. To overcome this particular restriction it can be very useful to complement the information obtained by EXAFS with that obtained with transmission electron microscopy, which apart from EXAFS can detect the smaller metal particles. In addition, TEM yields information of *each*

Table 3
Coordination numbers N_{Pt-Pt}, number of atoms per particle n_{atoms}, and particle diameter D (Å), for fully reduced samples [a]

	DECH350			R350			OR350		
Shell	N_{Pt-Pt}	n_{atoms}	D(Å)	N_{Pt-Pt}	n_{atoms}	D(Å)	N_{Pt-Pt}	n_{atoms}	D(Å)
1	7.2	40	13	10.1	650	35	5.5	14	9
2	2.8	40	13	4.4	360	27	2.0	19	11
3	8.8	40	13	17.5	650	35			

[a] Taken from Ref. [15].

individual metal particle, and thus it can provide particle size distributions. As an example, Fig. 7 includes the simulated micrographs of rhodium particles in an Rh/CeO_2 system [26] with increasing sizes of rhodium metal particles, being the smaller metal particles detected 10 Å in diameter.

In relation with the second point, for the particular case of supported metal particles several factors affecting the EXAFS function amplitude can be estimated, and thus, the uncertainty about coordination number can be minimized. The first one, S_0^2, the amplitude reduction factor, can be calibrated with the spectra of the corresponding metal foils, measured in the same conditions. There is a coupling between Debye–Waller factor and coordination numbers that in other systems yields several "best" fits, increasing or decreasing simultaneously both parameters. But for the special case

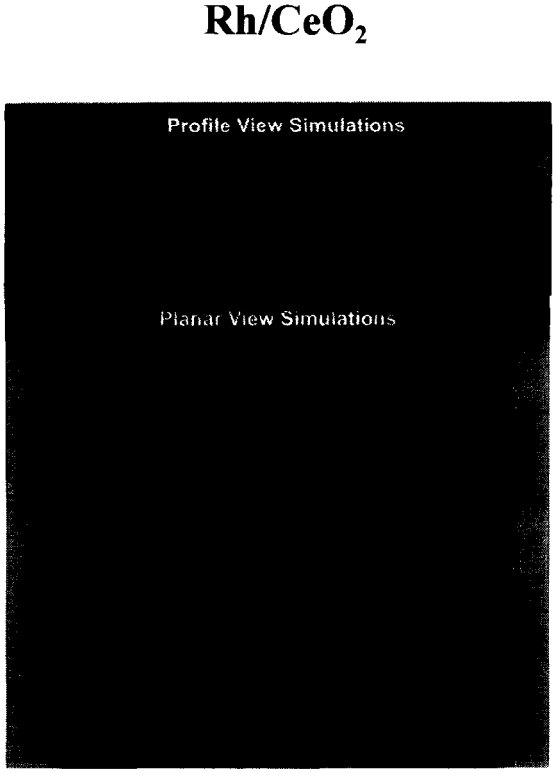

Fig. 7. Profile view (upper part) and planar view (lower part) of HRTEM simulations obtained for rhodium particles supported over CeO_2 at increasing metal particle sizes. (By courtesy of Prof. S. Bernal, University of Cadiz.)

of small metal particles, as already shown in the Pt/Al_2O_3 samples, both parameters should change in an opposite way: Debye–Waller factors should decrease, when coordination number increase, since when metal particles grow, metal atoms became more ordered.

The anharmonic contribution to the EXAFS function in small metal particles deserves particular attention, because it can yield to an underestimation of coordination numbers as high as 25% [23]. In standard EXAFS formulations harmonic pair distribution functions are assumed. Nevertheless, atoms in the surface region of the small metal particles move under anharmonic potential and, as a consequence, the pair distribution function becomes asymmetric, particularly for "soft" metals, such as copper. This anharmonic contribution is minimized when decreasing the recording temperature. When this is not possible, e.g. when recording in situ the EXAFS spectrum of a catalytic system, somewhat higher apparent coordination number could be obtained by allowing the Debye–Waller factor to be an adjustable parameter in the fits [12]. Alternatively, it can be accounted for calculating the amplitude $A(k)$ and phase shift $\Psi(k)$ functions using the cumulant expansion approach proposed by Bunker [27] as outlined below:

$$A(k) = \frac{N}{kR^2}F(k)e^{(-2R/\lambda(k))} \times \exp(-2k^2\sigma^2 + \tfrac{2}{3}C_4k^4 - \cdots), \quad (3)$$

$$\Psi(k) = 2kR + \phi(k) - \tfrac{4}{3}C_3k^3 + \cdots \quad (4)$$

being C_4, C_3,..., higher order cumulants which are a measure of the deviation of the pair distribution function from the Gaussian shape.

A metal–metal bond contraction for small metal particles was first reported by Apai et al. [24] and subsequently by many other authors [28]. Although it has a small effect in the fit parameters, on average a few hundredths of an angström in coordination distances and some authors have even detected an enlargement of metal–metal distances in supported metal catalyst, it deserves particular attention. Since this effect has been related primarily with surface anharmonicity, it could be dealt with introducing the cumulant expansion in the EXAFS formulation and, when possible, reducing

the recording temperature. All the above considerations are made for the equilibrium shape of free particles, i.e. in the absence of any interaction with gases and/or other phases.

In systems where the metal phase is not fully reduced, the actual and real coordination numbers of the oxidized species have to be known to calculate the real coordination number of the reduced metal particles [24]. Thus, further assumptions and calculations are needed in these systems.

6. Conclusions

The capabilities of the EXAFS technique make it a unique tool to determine metal particle sizes for particles with a diameter smaller than 15 Å. As with every other technique, there are limitations that have to be known to overcome them. Within the range 5 Å $< d <$ 15 Å a comparison with the results obtained by TEM can be made. Nevertheless, for the new supported metal clusters, where metal aggregates include 4–8 atoms, recently reviewed by Gates [29], EXAFS has no competitor.

Acknowledgements

The SRS (Daresbury Laboratory, UK) and LIP (EU) are acknowledged for beam time allocation and the Spanish DGICCYT (Project Number PB95-0549) for financial support. Prof. S. Bernal from the University of Cádiz is acknowledged for supplying Fig. 7.

References

[1] R. Prins, D.C. Koningsberger, in: D.C. Koningsberger, R. Prins (Eds.), X-Ray Absorption: Principles, Applications, Techniques of EXAFS, SEXAFS and XANES, Wiley/Interscience, New York, 1988, p. 321.
[2] R.B. Greegor, F.W. Lytle, J. Catal. 63 (1980) 476.
[3] K. Foger, Catalysis Science and Technology, in: J.R. Anderson, M. Boudart (Eds.), Ch. 4, Springer, Berlin, 1984.
[4] J.R. Anderson, Structure of Metallic Catalysis, Academic Press, New York. 1975.
[5] R.W. Joyner, Catal. Today 9 (1991) 161.
[6] P.G. Menon, G.F. Froment, Appl. Catal. 1 (1981) 31.
[7] S.J. Tauster, S.C. Fung, R.L. Garten, J. Am. Chem. Soc. 100 (1978) 170.
[8] P.J. Levy, M. Primet, Appl. Catal. 70 (1991) 263.
[9] K. Heinemann, F. Soria, Ultramicroscopy 20 (1986) 1.
[10] A.F. Wells, Structural Inorganic Chemistry, Oxford University Press, Oxford, 1975.
[11] R.E. Benfield, J. Chem. Soc. Faraday Trans. 88 (8) (1992) 1107.
[12] B.S. Clausen, L. Gråbaek, H. Topsøe, L.B. Hansen, P. Stoltze, J.K. Nørskov, O.H. Nielsen, J. Catal. 141 (1993) 368.
[13] A. Jentys, D.H. Gay, A.L. Rohl, Catal. Lett 30 (1995) 77.
[14] E.D. Crozier, A.J. Seary, M.K. McManus, D.T. Jiang, J. Phys. IV (France) 7 (1997) C2-251.
[15] A. Muñoz-Páez, D.C. Koningsberger. J. Phys. Chem. 99 (1995) 4193.
[16] A. Muñoz-Páez, R.R. Pappalardo, E. Sánchez-Marcos, J. Am. Chem. Soc. 117 (1995) 11710.
[17] S. Díaz-Moreno, A. Muñoz-Páez, J.M. Martínez, R.R. Pappalardo, E. Sánchez-Marcos, J. Am. Chem. Soc. 118 (1996) 12654.
[18] K.I. Pandya, S.M. Heald, J.A. Hriljac, L. Petrakis, J. Fraissard, J. Phys. Chem. 100 (1996) 5070.
[19] S.D. Jackson, M.B.T. Keegan, C.D. McLellan, P.A. Meheux, R.B. Moyes, G. Webb, P.B. Wells, R. Whyman, J. Willis, in: G. Poncelet, P.A. Jacobs, P. Grange, B. Delmon, (Eds.), Preparation of Catalysts V, Elsevier, Amsterdam, 1991, p. 135.
[20] B.J. Kip, F.B.M. Duivenvoorden, D.C. Koningsberger, R. Prins, J. Catal. 105 (1987) 26.
[21] F.W.H. Kampers, C.W.R. Engelen, J.W.C. Van Hooff, D.C. Koningsberger, J. Phys. Chem. 94 (1990) 8574.
[22] J.J. Rehr, J. Mustre de Leon, S.I. Zabinsky, R.C. Albers, J. Am. Chem. Soc. 113 (1991) 5135.
[23] B.S. Clausen, H. Topsøe, L.B. Hansen, P. Stoltze, J.K. Nørskov, Catal. Today 21 (1994) 49.
[24] P.W.J.G. Wijnen, F.B.M. Van Zon, D.C. Koningsberger, J. Catal. 114 (1988) 463.
[25] G. Apai, J.F. Hamilton, J. Stohr, A. Thompson, Phys. Rev. Lett. 43 (2) (1979) 165.
[26] S. Bernal, F.J. Botana, J.J. Calvino, M.A. Cauqui, G.A. Cifredo, A. Jobacho, J.M. Pintado, J.M. Rodríguez-Izquierdo, J. Phys. Chem. 97 (1993) 4118.
[27] G. Bunker, Nucl. Instr. Meth. 207 (1983) 437.
[28] J.C.J. Bart, G. Vlaic, Adv. in Catal. 35 (1987) 1.
[29] B.C. Gates, Chem. Rev. 95 (1995) 511.